Conformational Equilibria of Peroxynitrous Acid in Water: A First-Principles Molecular Dynamics Study

Karel Doclo and Ursula Rothlisberger*,†

Laboratory of Inorganic Chemistry, ETH Zentrum, CH-8092 Zurich, Switzerland

Received: March 30, 2000

An aqueous solution of peroxynitrous acid has been studied using first-principles molecular dynamics simulations based on density functional theory. The relative Helmholtz energies of different conformers have been determined via thermodynamic integration with constraints. At contrast to the gas phase, only two conformers, a *cis* and a *trans* isomer, are present in solution and their relative Helmholtz energy is enhanced with respect to the gas phase. The average structural properties of the two conformational forms on the other hand are very close to the respective gas phase values. The interconversion pathway between the two conformers has been determined, and the Helmholtz energy profile for the isomerization reaction in solution is presented. The rotational barrier is calculated to be substantially higher than in gas phase due to a strong rearrangement of the solvent during the reaction. The structure of the transition state can only be described correctly when the solvent is taken explicitly into account. Our calculations indicate that the *cis* form is the dominant species in aqueous solution at ambient temperatures.

1. Introduction

Under physiological conditions, peroxynitrous acid (hydrogen oxoperoxonitrate, ONOOH) is in equilibrium with peroxynitrite ($ONOO^-$), which is generated in vivo through the reaction of nitric oxide and superoxide.[1] Whereas $ONOO^-$ is very stable in basic solutions, ONOOH has a lifetime of only about 3 s at 25 °C and neutral pH.[2] In the absence of any substrate, peroxynitrous acid isomerizes spontaneously to nitric acid. On the other hand, ONOOH is known to attack a variety of biological targets such as DNA,[3] methinonine,[4] and lipids,[5] as a potent oxidant. Two different oxidation reactions have been observed involving one and two electron processes, respectively. The latter takes place via a direct bimolecular reaction between ONOOH and the reductant,[6] whereas the former appears to involve at least two intermediates along the reaction pathway, from which only one is acting as an oxidant.[5,7] The nature of the reactive species is still a point of controversy, and several hypotheses have been suggested during the last years. Reactivity has been assigned to free $^{\bullet}OH$ and $^{\bullet}NO_2$ radicals produced by homolysis of the peroxy bond,[8,9] to caged radical pairs,[10] to an unidentified high-energy activated species, $ONOOH^*$, formed along the reaction coordinate for the *cis*−*trans* isomerization,[7] or to the *trans* isomer of ONOOH.[6,11]

Despite the existence of a large body of experimental data, the chemistry of peroxynitrous acid is still poorly understood. In view of the role of ONOOH as a potentially harmful biological oxidant, several quantum chemical studies have been carried out to characterize this intriguing system in more detail. On the basis of gas-phase calculations, Houk et al.[12] proposed two hydrogen-bonded diradicals for the activated form of peroxynitrous acid, ONOOH*, with an energy of 71 kJ/mol above that of ONOOH. The existence of these structures in aqueous solution, however, is questionable. Alternatively, different conformational forms have been invoked as an explanation of the high reactivity of ONOOH. Peroxynitrous acid can form different conformers that are characterized by two dihedral angles, i.e., τ(ONOO) and τ(NOOH). Angles near 0, 90, and 180° are usually designated as *cis*, *perp*, and *trans*, respectively. For the gas phase, McGrath and Rowland[13] have found three almost isoenergetic minima, *cis*−*cis*, *cis*−*perp*, and *trans*−*perp*, with the *cis*−*cis* having the lowest energy. This result was subsequently confirmed by several other groups.[12,14,15] The barrier corresponding to the conversion of the *cis* conformer into the *trans* conformer by a rotation around the central N−O bond is estimated to be roughly 55 kJ/mol.[13−15] Through the comparison of experimental[16] and calculated[13] spectra, it was concluded that the conformer observed in matrix isolation experiments is the *trans* form. In contrast, the synthesis of peroxynitrite via nitrogen monoxide gas and tetramethylammonium superoxide yields exclusively *cis*-peroxynitrite,[17] and we have recently suggested a possible explanation for the strong preference of the *cis* isomer on the basis of intrinsic differences in the electronic structure.[15]

Until now, all theoretical investigations refer to the gas phase, in contrast to the biorelevant chemistry in aqueous solution. Tsai et al.[14] made a first attempt to take solvent effects into account for the peroxynitrite anion, using a self-consistent isodensity−polarizability continuum model.

First-principles molecular dynamics (MD) simulations, as proposed by Car and Parrinello,[18] offer an interesting alternative approach that allows for an explicit description of the solvent. This recent method is able to describe the details of the motion of the solute as well as the finite-temperature solvent dynamics. These kinds of simulations have proven to be a valuable tool for an accurate first-principles description of water and aqueous solutions.[19−22] In this work, we use ab initio molecular dynamics to characterize the conformational equilibria of peroxynitrous acid in aqueous solution. We have performed Helmholtz energy calculations of the relative stability of different conformers and their interconversion pathway. The influence of the explicit inclusion of the solvent will be discussed in detail.

† E-mail: uro@inorg.chem.ethz.ch.

10.1021/jp0012193 CCC: $19.00
Published on Web 06/20/2000

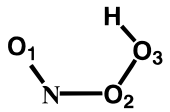

Figure 1. Labeling scheme of the oxygen atoms in ONOOH.

2. Computational Details

The method of first-principles molecular dynamics, as used in this study, was proposed by Car and Parrinello in 1985.[18] These simulations combine a classical MD scheme with an electronic structure calculation in the framework of density functional and pseudopotential theory. We performed gradient corrected calculations with the functional developed by Becke[23] for the exchange and by Lee, Yang, and Parr[24] for the correlation part (BLYP), which is particulary well suited for the description of water[25] and aqueous solutions.[20−22] Kohn−Sham orbitals are expanded in plane waves up to an energy cutoff of 70 Ry, which is sufficient to yield converged structural properties for water[25] and for the solute ONOOH.[15] As the density of a peroxynitrous acid solutions is likely to be very close to water, we have chosen the size of our system around a density of 1 g/mL with the additional two conditions that a ONOOH molecule is at least surrounded by two coordination shells of solvent and that the diffusion coefficient of the solvent is close to the one obtained for pure water. These criteria could be fulfilled with a system containing 1 ONOOH and 52 H_2O molecules in a periodic simple cubic cell of size $a = 12.00$ Å. We used the same soft pseudopotentials of the Martins−Trouiller type[26] as in our previous gas-phase study,[15] with cutoff radii r_{cs} of 0.5 au for hydrogen, r_{cs} and r_{cp} of 1.12 au for nitrogen and, r_{cs} and r_{cp} of 1.11 au for oxygen. Hydrogen nuclei are treated as classical particles with the mass of the deuterium isotope. The effective mass determining the time scale of the fictitious dynamics of the electrons is 1000 au. The equations of motion are solved using a velocity Verlet integrator with a time step of 7 au (0.169 fs). We have performed constant volume−constant temperature simulations in which the average temperature of the sample is 300 K. In the initial stage of the MD run, the temperature of the ions is controlled by velocity rescaling. After an equilibration time of ≃0.5 ps, the run is continued for another ∼6 ps with a Nosé−Hoover thermostat,[27] acting on the ionic degrees of freedom. Calculations of the relative Helmholtz energies along the *cis*−*trans* isomerization pathway are performed via thermodynamic integration.[28] Average values of the Lagrange multipliers were determined for a discrete set of dihedral angles τ(ONOO) by performing a constrained MD run for each of these states. The total simulation time of all 8 points adds up to ∼50 ps. All calculations are performed with the program CPMD.[29]

3. Results and Discussion

3.1. Structural Properties of the Different Conformers. A quantitative analysis of the average structural properties can be obtained from the radial distribution functions. Figure 1 gives the labeling scheme we have used for peroxynitrous acid. Upon analysis of the various pair correlation functions for the *cis* and *trans* isomers, it becomes apparent that the molecule consists of a hydrophilic and a hydrophobic part. As shown in Figure 2, O^3 and H have hydrophilic character. Although noisy due to the limited statistics (there is only one ONOOH molecule present in the simulation box), one can clearly see that the radial pair correlation function g_{HO_w} of the terminal hydrogen of peroxynitrous acid with the oxygen of the solvent (O_w) has a first peak centered around 1.65 Å for the *cis* and around 1.73 Å for the *trans* isomer, i.e., in the range of typical hydrogen-bonded H−O

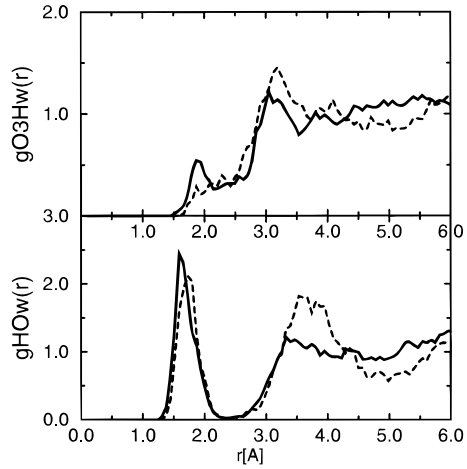

Figure 2. Radial distribution functions, as obtained from ab initio MD simulations at 300 K using the BLYP exchange correlation functional. Continuous lines stand for the *cis* conformer; dashed lines, for the *trans* conformer.

distances. The donor−acceptor distance is shorter than in pure water, where the hydrogen-bonded peak occurs around 1.85 Å.[25,30] This indicates that the hydrogen bond formed by the terminal hydrogen is strong, i.e., the terminal proton is acidic. The coordination number integrated up to the minimum beyond the first peak is 1.0 for both conformers. The terminal hydrogen atom thus forms an intermolecular hydrogen bond at any instant in time for both the *cis* and the *trans* conformers. Due to this high strength of the hydrogen bond to the solvent, the conformer calculated to be the most stable one in gas phase, i.e., *cis,cis*-ONOOH which has an intramolecular hydrogen bond, does not occur in solution. The radial distribution functions for O^3, the oxygen bound to the terminal hydrogen, are more distinct for both conformers. In the case of the *cis* conformer, there is a small peak around 1.85 Å whereas for *trans*-ONOOH this peak is turned into a broad shoulder around 1.8−2.4 Å. Integration up to the first minimum gives a value of 0.6−0.7 for both isomers. The longer range parts of the pair-correlation functions $g_{O^3H_w}$ and g_{HO_w} are more structured for the *trans* conformer. This is likely due to the build up of a hydrogen-bonded intermolecular bridge: the water molecule that makes a hydrogen bond with the terminal hydrogen atom is also linked to the O^3 atom.

Figure 3 shows the pair correlation functions for O^1, N, and O^2. In all three cases, the typical hydrogen-bonded peak around 1.85 Å is missing, indicating that these atoms are hydrophobic and cause the formation of a solvent cage. The distance up to which no net probability density is found gives an indication of the cage size, i.e., the space around the peroxynitrous acid where no water molecules are found. As can be seen from Figure 3, this distance is ≃2.0 Å for the *cis* and the *trans* conformers, with the cage being slightly larger for the latter.

A comparison with the results obtained from gas-phase calculations can be made from the averaged structures for the two conformers in solution. All values are listed in Table 1. Angles have been omitted because the difference between all calculations does not exceed 1°. As mentioned before, the *cis*−*cis* conformer is not present in solution: *cis* and *trans* thus correspond to *cis*−*perp* and *trans*−*perp* in the gas phase. It can clearly be seen that the averaged structures do not change drastically upon the explicit inclusion of the solvent: the $N-O^2$ bond is shortened by 0.06 Å for the *cis* conformer, whereas the O^2-O^3 bond is a bit longer and the O^1-N bond remains essentially constant. A major change for the *trans* isomer

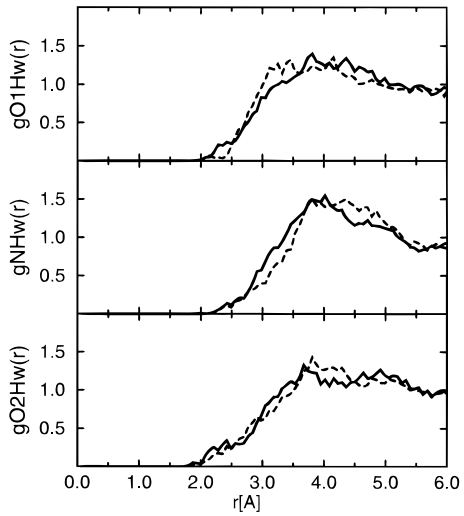

Figure 3. Radial distribution functions, as obtained from ab initio MD simulations at 300 K. Continuous lines stand for the *cis* conformer; dashed lines, for the *trans* conformer.

TABLE 1: Averaged Solution Geometries of the *Cis* and *Trans* Conformers of ONOOH in Comparison with the Optimized Geometries in the Gas Phase with Distances in Å and Dihedral Angles in deg

	cis-ONOOH			*trans*-ONOOH		
	solvent	DFT[a]	MP2[b]	solvent	DFT[a]	MP2[b]
$d(O^1-N)$	1.18	1.16	1.17	1.18	1.17	1.16
$d(N-O^2)$	1.55	1.61	1.49	1.58	1.60	1.53
$d(O^2-O^3)$	1.49	1.46	1.42	1.48	1.47	1.42
$d(O^3-H)$	1.01	0.98	0.97	1.02	0.98	0.97
τ(ONOO)	7.1	4.4	3.6	173.8	185.3	183.7
τ(NOOH)	78.5	96.5	104.3	108.2	108.5	103.5

[a] Reference 15, with the same theoretical approach. [b] Reference 14.

involves the dihedral angle τ(ONOO), which is on average $\simeq 10°$ larger in solution.

3.2. Structures along the Isomerization Pathway. The reaction coordinate for the *cis*−*trans* isomerization is defined by the dihedral angle τ(ONOO). Detailed information about the structure of ONOOH and the surrounding solvent along this reaction coordinate is given by the change of the radial distribution functions. The most drastic changes are observed for $g_{O^2H_w}$ (Figure 4) while all the other pair correlation functions remain essentially similar. When the transition state is approached, corresponding to a dihedral angle of $\tau = 90°$, a hydrogen-bonded peak centered around 1.7 Å is built up, indicating that the solvent cage, which is clearly present in the equilibrium *cis* and *trans* structures, is partially broken down. This is nicely illustrated in Figure 5, which shows the highest occupied Kohn−Sham orbital (HOMO) of the system, a well localized antibonding π-orbital. The atoms O^2, O^3, and the terminal hydrogen form a hydrogen bond with the surrounding water, whereas the atoms O^1 and N are situated in a cage. At the transition state, the average coordination number of the oxygen atom O^2 has a value of 1.0. At the same point, the O^2-H_w distribution is only about 0.1−0.2 for the equilibrium *cis* and *trans* forms and about 0.4 for the structures corresponding to dihedral angles τ(ONOO) of 60 and 120°.

The O^3-H_w pair correlation function is much less structured at the transition state than in the end points of the reaction pathway. In contrast, the O^1 and N atoms keep their hydrophobic character throughout the isomerization. The same holds for the hydrophilicity of the terminal hydrogen atom, which stays always bound to the O^3 oxygen atom of peroxynitrous acid.

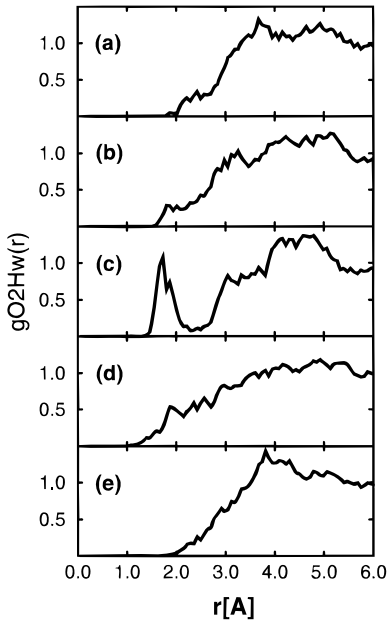

Figure 4. O^2-H_w radial distribution function, as obtained from an ab initio MD calculation at 300 K: (a) τ(ONOO) of the *cis* conformer; (b) τ(ONOO) = 60°; (c) τ(ONOO) = 90°; (d) τ(ONOO) = 120°; (e) τ(ONOO) of the *trans* conformer.

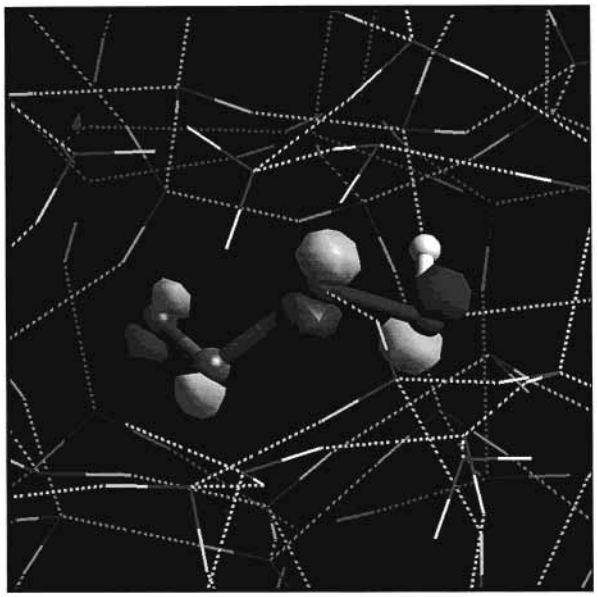

Figure 5. Contour plot of the highest occupied Kohn−Sham orbital at the transition state for *cis*−*trans* isomerization.

TABLE 2: Structural Properties of Liquid Water

	BLYP	BLYP[a]	expt[b]
r_{OO}^{max} (Å)	2.80	2.80	2.85
g_{OO}^{max}	2.80	2.40	3.10
r_{OO}^{min} (Å)	3.40	3.35	3.27
g_{OO}^{min}	0.60	0.80	0.73
n_c	4.2	4.5	4.5

[a] Reference 25. [b] Reference 30.

Table 2 shows the variation of the most important distances for different dihedral angles τ(ONOO) in comparison to the gas phase. The only distance that is changing substantially is the $d(N-O^2)$ which is considerably weakened due to the loss of the $N-O^2$ π-bond at τ(ONOO) = 90°.[31] The lengthening is more

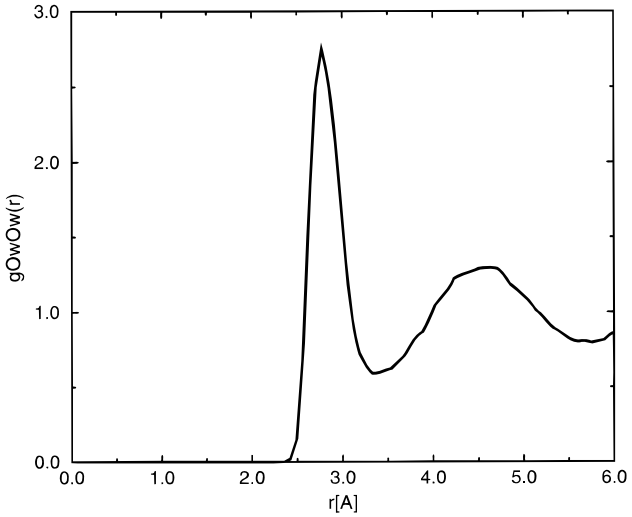

Figure 6. Radial oxygen−oxygen distribution function for the water solvent, as obtained from ab initio MD simulations at 300 K using the BLYP exchange correlation functional.

TABLE 3: Averaged Distances in Å for ONOOH at Different Dihedral Angles τ(ONOO)[a]

	$d(O^1-N)$	$d(N-O^2)$	$d(O^2-O^3)$
cis conformer	1.18 (1.16)	1.55 (1.61)	1.49 (1.46)
τ(ONOO) = 40°	1.17	1.64	1.48
τ(ONOO) = 60°	1.16	1.71	1.48
τ(ONOO) = 90°	1.15 (1.16)	1.81 (1.70)	1.48 (1.49)
τ(ONOO) = 120°	1.16	1.74	1.48
τ(ONOO) = 150°	1.18	1.63	1.48
trans conformer	1.18 (1.17)	1.58 (1.60)	1.48 (1.47)

[a] Values for the gas phase are given in parentheses. Only the structural parameters which vary significantly during the isomerization are tabulated.

pronounced in solution (Δd = 0.25 Å) than in the gas phase (Δd = 0.10 Å). This enhanced bond elongation in solution is most likely a consequence of the formation of a hydrogen bond between O^2 and a close water molecule, as discussed above. From these results, it is clear that gas-phase calculations cannot give a satisfactory description of the transition state of the *cis*−*trans* isomerization reaction in solution. Also the inclusion of solvent effects with a continuum model would fail to describe the transition state properly.

An additional result of our calculation is the solvent−solvent pair correlation functions for H_2O, i.e., g_{OO}, g_{OH}, and g_{HH}. These functions are very similar with the ones obtained in previous ab initio MD simulations of pure water,[25] indicating that the chosen sample size is big enough to reproduce essentially bulk properties of the surrounding solvent. As an example, the g_{OO} pair correlation function obtained from our calculations is shown in Figure 6. Table 3 shows a comparison of the structural parameters for g_{OO}. The coordination number n_c is obtained through the integration of g_{OO} over a sphere with radius r_c, which is the location of the first minimum in the O−O radial distribution function. The presence of one ONOOH molecule in our simulation box can explain the slightly lower coordination number n_c and may also be responsible for the fact that the radial distribution function is a little overstructured. However, the overall agreement is very good, indicating that the surrounding solvent is essentially bulk water.

3.3. Energetics. The relative Helmholtz energies are obtained through thermodynamic integration, a technique developed for classical MD simulations. This approach uses the method of constraints to determine the mean force f that is necessary to keep the system at a given point of the reaction coordinate c. The average constrained force is determined for a series of different values c' of the reaction coordinate, and the relative Helmholtz energies ΔF are obtained by integration, i.e.

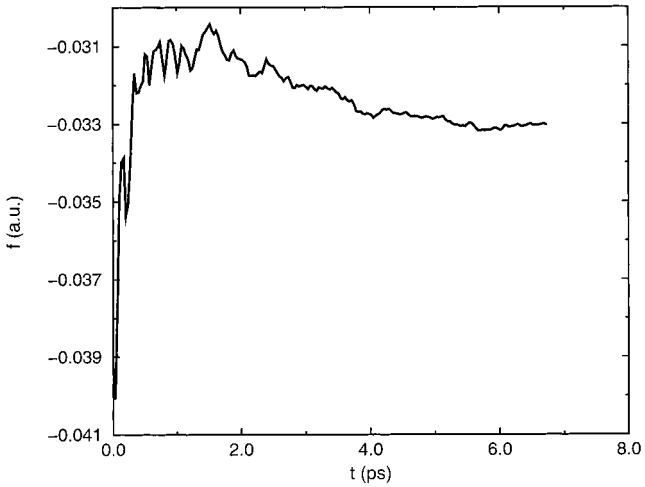

Figure 7. Running average of the Lagrange multiplier for a constrained ab initio MD simulation of ONOOH with τ(ONOO) = 40° at 300 K.

$$\Delta F(c) = F(c) - F(c_0) = -\int_{c_0}^{c} dc'\, f(c') \qquad (1)$$

In an ab initio MD implementation, the mean force is equal to the corresponding Lagrange multiplier $\lambda(c)$ with an additional compensating term that arises from constraining the reaction coordinate.[28] We did not take the latter explicitely into account because the correction is in general not significant[28,32] and smaller than the statistical errors in our calculations.

The reaction coordinate corresponding to the *cis*−*trans* isomerization is the dihedral angle τ(ONOO). We evaluated the average Langrange multiplier $\lambda(\tau)$ for a series of values of τ, varying from τ(ONOO) ≃7° to $\tau(ONOO)_{trans}$ ≃174°. The final state of the previous simulation is always used as the initial configuration of the next one. Finally, the relative Helmholtz energies for the set of τ values are obtained as a discrete approximation to the integral

$$\Delta F(\tau) = -\int_{\tau_0}^{\tau} d\tau' \,\langle\lambda(\tau')\rangle \qquad (2)$$

To obtain accurate Helmholtz energies, it is necessary to have a sufficiently long sampling time at a given value of the constrained reaction coordinate. Figure 7 shows the running average for the Lagrange multiplier $\langle\lambda\rangle$, corresponding to a dihedral angle τ(ONOO) of 40°, as a representative example. The value has converged after ≃6 ps. The same sampling time was used for the other points along the reaction pathway.

The averaged Lagrange multipliers along the reaction pathway, together with their error bars calculated as the standard deviation of the average value of $\lambda(\tau)$ for windows of 34 fs, are plotted in Figure 8, and the corresponding Helmholtz[2] energy profile is shown in Figure 9. [Calculated Helmholtz energies are likely to be similar to the experimentally measured Gibbs energies, because the pressure term $p\Delta V$ is expected to be small, due to the incompressibility of water.] The value of $\langle\lambda\rangle$ changes very rapidly around the conformational minima. To determine the origin of this effect, we made the same calculations in gas phase and found that this behavior is intrinsic to the ONOOH molecule. During the *cis*−*trans* isomerization, the π-bond between N and O^2 (corresponding to the HOMO-2) is broken.

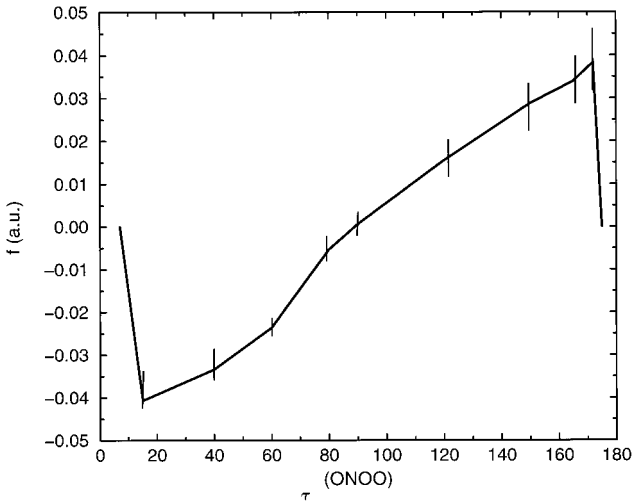

Figure 8. Averaged Lagrange multipliers along the reaction pathway as obtained from constrained ab initio MD simulations for ONOOH at 300 K.

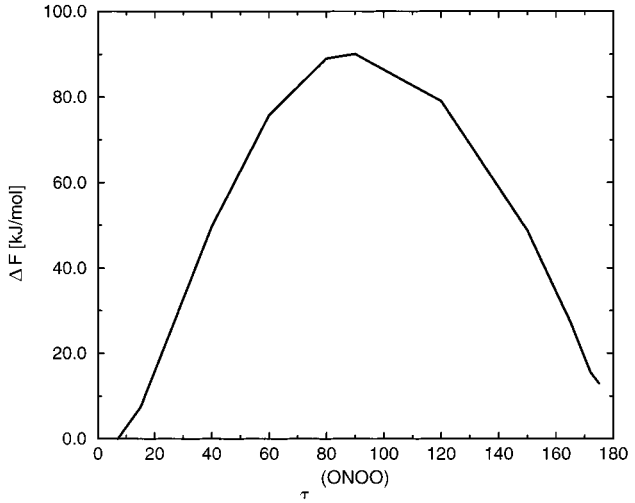

Figure 9. Helmholtz energy profile in function of τ(ONOO) from constrained ab initio MD simulations for ONOOH at 300 K, relative to the Helmholtz energy for τ(ONOO) = 7°.

Already a small change in the dihedral angle τ(ONOO) is accompanied with a drastic decrease in the overlap of the adjacent *p*-orbitals. Thus the breaking of the N−O^2 π-bond occurs essentially in the first few degrees along the reaction coordinate. The Helmholtz energy of the *trans* isomer is found to be 15 ± 5 kJ/mol higher than the *cis* isomer, which corresponds to an equilibrium distribution greater than 200:1 for the ratio of *cis* to *trans* in solution at 300 K. This value is larger than the ones found in the gas phase; using the same formalism as in this study, we calculated previously[15] an energy difference of 9.7 kJ/mol for the corresponding *cis*−*perp* and *trans*−*perp* conformers at 0 K, in agreement with other gas-phase studies with values between 6.7 and 9.7 kJ/mol [13,14] depending on the level of theory used.

For the barrier corresponding to the *cis*−*trans* isomerization, a substantially larger value than in the gas phase is found. Without solvent, this barrier is calculated to be roughly 55 kJ/mol,[13−15] whereas in solution the energy needed to convert the *cis* isomer into the *trans* isomer is as high as 89 ± 10 kJ/mol. Interestingly, this coincides with the activation enthalpy for the isomerization of peroxynitrous acid to nitric acid.[33] Although the transition state in aqueous solution is stabilized through the formation of a hydrogen bond, the activation energy for *cis*−*trans* isomerization turns out to be higher than in the gas phase. One possible rationale for this observation is the fact that the weakening of the N−O^2 bond in the transition state is more pronounced in the presence of the solvent leading to an overall decrease of stability for the activated complex. Furthermore, the entropic penalty due to the large rearrangement of the surrounding solvent that occurs during the isomerization reaction clearly plays a decisive role for the total energetics in solution. On the basis of these results, we can conclude that, in aqueous solution, the *cis* isomer is the dominant form at ambient temperature.

4. Conclusions

In aqueous solution, peroxynitrous acid has been found to have a hydrophilic part, i.e., the terminal OH unit, and a hydrophobic part, i.e., the ONO unit, which causes the formation of a solvent cage. It has also been shown that, in contrast to the gas phase, only two conformational forms exist in solution, a *cis* and a *trans* conformer with the former being the dominant one. The relative energy difference between the *cis* and *trans* conformer ($\Delta F = 15 \pm 5$ kJ/mol) is enhanced with respect to the gas phase. Solvent effects on the structural parameters on the other hand are relatively small. The investigation of the *cis*−*trans* isomerization pathway shows a strong restructuring of the solvent shell at the transition state that can only be taken into account by an explicit solvent model, as used in this work. Due to the additional solvent reorganization, the barrier for *cis*−*trans* isomerization is with 89 ± 10 kJ/mol substantially higher than in the gas phase.

Acknowledgment. We thank W. H. Koppenol for suggesting this study and for a careful reading of the manuscript. We are also grateful to M. Sprik for many useful discussions and to P. Maurer for the analysis of the Kohn−Sham orbitals of ONOOH in the gas phase.

References and Notes

(1) Beckman, J. S.; Beckman, T. W.; Chen, J.; Marshall, P. A.; Freeman, M. A. *Proc. Natl. Acad. Sci. U.S.A.* **1990**, *87*, 1620.
(2) Koppenol, W. H.; Kissner, R. *Chem. Res. Toxicol.* **1998**, *11*, 87.
(3) King, P. A.; Anderson, V. E.; Edwards, J. O.; Gustafson, G; Plus, R. C.; Suggs, J. W. *J. Am. Chem. Soc.* **1992**, *114*, 5430.
(4) Pryor, W. A.; Jin, X.; Squadrito, G. L. *Proc. Natl. Acad. Sci. U.S.A.* **1994**, *91*, 11173.
(5) Radi, R.; Beckman, J. S.; Bush, K. M.; Freeman, B. A. *J. Biol. Chem.* **1991**, *266*, 4244.
(6) Goldstein, S.; Czapski, G. *Inorg. Chem.* **1995**, *34*, 4041.
(7) Koppenol, W. H.; Moreno, J. J.; Pryoir, W. A.; Ischiropoulos, H.; Beckman, J. S. *Chem. Res. Toxicol.* **1992**, *5*, 834.
(8) Merenyi, G.; Lind, J. *Chem. Res. Toxicol.* **1997**, *10*, 1216.
(9) Goldstein, S.; Czapski, G. *J. Am. Chem. Soc.* **1998**, *120*, 3458.
(10) Pryor, W. A.; Squadrito, G. L. *Am. J. Physiol.* **1995**, *268*, L699.
(11) Goldstein, S.; Meyerstein, D.; van Eldik, R.; Czapski, G. *J. Phys. Chem. A* **1997**, *101*, 7114.
(12) Houk, K. N.; Condroski, K. R.; Pryor, W. A. *J. Am. Chem. Soc.* **1996**, *118*, 13002.
(13) McGrath, M. P.; Rowland, F. S. *J. Phys. Chem.* **1994**, *98*, 1061.
(14) Tsai, H. H.; Hamilton, T. P.; Tsai, J. H. M.; van der Woerd, M.; Harrison, J. G.; Jablonsky, M. J.; Beckman, J. S.; Koppenol, W. H. *J. Phys. Chem.* **1996**, *100*, 15087.
(15) Doclo, K.; Rothlisberger, U. *Chem. Phys. Lett.* **1998**, *297*, 205.
(16) Cheng, B. M.; Lee, J. W.; Lee, Y. P. *J. Phys. Chem.* **1991**, *95*, 2814.
(17) Wörle, M.; Latal, P.; Kissner, R.; Nesper, R.; Koppenol, W. H. *Chem. Res. Toxicol.* **1999**, *12*, 305.
(18) Car, R.; Parrinello, M. *Phys. Rev. Lett.* **1985**, *55*, 2471.
(19) Tuckerman, M.; Laasonen, K.; Sprik, M.; Parrinello, M. *J. Chem. Phys.* **1995**, *103*, 150.
(20) Curioni, A.; Sprik, M; Andreoni, W.; Schiffer, H.; Hutter, J.; Parrinello, M. *J. Am. Chem. Soc.* **1997**, *119*, 7218.

(21) Meijer, E. J.; Sprik, M. *J. Phys. Chem. A* **1998**, *102*, 2893.
(22) Brugé, F.; Bernasconi, M.; Parrinello, M. *J. Chem. Phys.* **1998**, *110*, 4734.
(23) Becke, A. D. *Phys. Rev. A* **1988**, *38*, 3098.
(24) Lee, C.; Yang, W.; Parr, R. G. *Phys. Rev. B* **1988**, *37*, 785.
(25) Sprik, M.; Hutter, J.; Parrinello, M. *J. Chem. Phys.* **1996**, *105*, 1142.
(26) Trouiller, N.; Martins, J. L. *Phys. Rev. B* **1991**, *43*, 1993.
(27) Tuckerman, M. E.; Parrinello, M. *J. Chem. Phys.* **1994**, *101*, 1302, 1316.
(28) Sprik, M.; Ciccotti, G. *J. Chem. Phys.* **1998**, *109*, 7737.
(29) CPMD written by Jürg Hutter, Max Planck Institut für Festkörperforschung, Stuttgart, Germany, 1995, with the help of the group for numerical intensive computations of IBM research Laboratory Zurich and the Abteilung Parrinello of the MPI Stuttgart.
(30) Soper, A. K. *J. Chem. Phys.* **1994**, *101*, 6288.
(31) An analysis of the Kohn−Sham one-electron orbitals of the gas-phase molecule shows that the molecular orbitals that contribute to the $N-O^2$ bond can be classified as a binding and an antibinding σ-type orbital and a binding π-orbital. This explains why despite the presence of a π-orbital the overall character of the $N-O^2$ bond is that of a single bond.
(32) Depaepe, J. M.; Ryckaert, J. P.; Paci, E.; Ciccotti, G. *Mol. Phys.* **1993**, *79*, 515.
(33) Padmaja, S.; Kissner, R.; Bounds, P. L.; Koppenol, W. H. *Helv. Chim. Acta* **1998**, *81*, 1201.